Available online at www.sciencedirect.com
SCIENCE DIRECT®
Journal of Theoretical Biology 230 (2004) 261–270
Journal of Theoretical Biology
www.elsevier.com/locate/jtbi

Propagation of electromagnetic radiation in mitochondria?

Roland Thar*, Michael Kühl

Marine Biological Laboratory Helsingør, University of Copenhagen, Strandpromenaden 5, Helsingør 3600, Denmark

Received 20 February 2004; received in revised form 12 May 2004; accepted 13 May 2004

Available online 17 July 2004

Abstract

Mitochondria are the main source of ultra-weak chemiluminescence generated by reactive oxygen species, which are continuously formed during the mitochondrial oxidative metabolism. Vertebrate cells show typically filamentous mitochondria associated with the microtubules of the cytoskeleton, forming together a continuous network (mitochondrial reticulum). The refractive index of both mitochondria and microtubules is higher than the surrounding cytoplasm, which results that the mitochondrial reticulum can act as an optical waveguide, i.e. electromagnetic radiation can propagate within the network. A detailed analysis of the inner structure of mitochondria shows, that they can be optically modelled as a multi-layer system with alternating indices of refraction. The parameters of this multi-layer system are dependent on the physiologic state of the mitochondria. The effect of the multi-layer system on electromagnetic radiation propagating along the mitochondrial reticulum is analysed by the transfer-matrix method. If induced light emission could take place in mitochondria, the multi-layer system could lead to lasing action like it has been realized in technical distributed feedback laser. Based on former reports about the influence of external illumination on the physiology of mitochondria it is speculated whether there exists some kind of long-range interaction between individual mitochondria mediated by electromagnetic radiation.

Keywords: Ultra-weak chemiluminescence; Optical waveguide; Mitochondrial reticulum; Reactive oxygen species (ROS); Refractive index

1. Introduction

The internal organization of eukaryotic cells is characterized by the compartments of diverse organelles (e.g. nucleus, endoplasmic reticulum, mitochondria, microsomes), which are related to specific physiological functions. The compartments are generally enclosed by one or two membranes consisting of a lipid bilayer. The membranes show diverse morphologies, ranging from simple spherical to highly complex configurations. Mitochondria consist of an outer membrane enclosing an inner membrane, which exhibits a complex pattern of invaginations called cristae. Different cell types show a wide variety of cristae morphologies, e.g. tubular, lamellar, helical, or even triangular cristae (Fawcett, 1981; Tandler and Hoppel, 1972). Vertebrate tissues typically show lamellar or tubular cristae, which are arranged perpendicular to the mitochondrial long axis yielding to a cross-striated appearance of the mitochondrion (Fawcett, 1981; Perkins and Renken, 1997; Riva et al., 2003; Tandler and Hoppel, 1972). The basic structure of mitochondria is closely related to their physiological function as the "power-house" of the cell. The oxidation of reduced substrates with molecular oxygen builds up a proton motive force across the inner membrane. The proton motive force is in turn utilized by membrane bound enzymes (Mitchell, 1977), which phosphorylate adenosine diphosphate (ADP) to adenosine triphosphate (ATP) the latter being the universal energy-providing molecule for biochemical reactions. In recent years mitochondria regained much research interest as their central role in programmed cell death (apoptosis) and in many diseases became evident (for a review see Nieminen, 2003; Ohta, 2003).

Despite the general "text book"-appearance of mitochondria as ovoid organelles of about 0.5 μm in diameter and 1 μm in length which originated from observations on isolated mitochondria, improved techniques in light microscopy such as differential interference contrast (DIC) and the application of fluorescent probes (Bereiter-Hahn, 1990; Bereiter-Hahn and Vöth,

*Corresponding author. Tel.: +45-4921-3344; fax: +45-4926-1165.
E-mail address: rthar@zi.ku.dk (R. Thar).

0022-5193/$ - see front matter © 2004 Elsevier Ltd. All rights reserved.
doi:10.1016/j.jtbi.2004.05.021

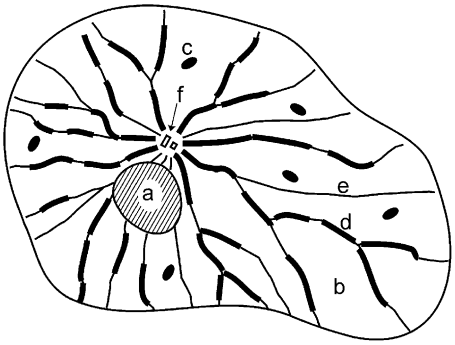

Fig. 1. Schematical drawing of a fibroblast in cell culture showing the radial organisation of microtubules and mitochondria centered around the centrosome. (a) Cell nucleus, (b) cytoplasm, (c) oval mitochondrion, (d) filamentous mitochondria, (e) microtubules, (f) centrosome.

1994) have shown that vertebrate mitochondria within intact cells of muscular, neuronal, or connective tissue are predominantly filamentous. Single filamentous mitochondria are typically about 100–500 nm in diameter and up to 10 μm in length, and they are associated with microtubules in the cytoskeleton (Ball, 1982; Heggeness et al., 1978). Microtubules and filamentous mitochondria form together complex reticula (networks) radiating from the centrosome (Fig. 1). Mitochondrial reticula have been observed in cell cultures of mammal fibroblasts, rat smooth muscle cells, rat sensory neurons, rat kidney cells, mouse macrophages, monkey myocardial cells, and *Xenopus* endothelial cells (Bakeeva et al., 1978; Bereiter-Hahn and Vöth, 1994; De Giorgi et al., 2000; Dedov and Roufogalis, 1999; Kirkwood et al., 1986; Poot et al., 1996; Shimada et al., 1984). Within muscle tissue these reticula actually extend across neighbouring cells resulting in a supracellular mitochondrial network as e.g. observed in the rat diaphragm muscle (Bakeeva et al., 1978).

Ultra-weak chemiluminescence appears as a general feature of all living organisms. It appears as a permanent weak light emission throughout the ultra-violet (UV), visible, and near-infrared (NIR) parts of the electromagnetic spectrum, which can be only detected by highly sensitive photo-multiplier-tubes (Cadenas, 1988; Inaba, 1988; Mei, 1994). Generally it is assumed that this light emission is linked to radical production accompanying the cell's metabolism (Adam and Cilento, 1982; Cilento and Adam, 1995). Radical production takes predominantly place in mitochondria, where redox-reactions of the mitochondrial respiration chain permanently produce reactive oxygen species (ROS) (Barja, 1999; Møller, 2001; Turrens, 2003). It was estimated that under normal conditions 1–2% of the cell's oxygen consumption is converted into ROS (Turrens, 2003). This level of ROS-production is essential for the physiological control of a variety of cell functions (Droge, 2002), whereas pathological increased levels of ROS cause oxidative damage to many cell compounds (Turrens, 2003). Several chemical mechanisms have been proposed to explain how ROS can generate electronic excited compounds (e.g. singlet oxygen or excited carbonyls), which are the source of chemiluminescence (Adam and Cilento, 1982; Cadenas, 1988; Cilento and Adam, 1995). Ultra-weak chemiluminescence has been directly measured from respiring isolated mitochondria, where peroxidation of mitochondrial membrane lipids was the presumable light-producing mechanism (Hideg et al., 1991). Specific substrates were shown to increase mitochondrial chemiluminescence significantly, as was demonstrated for the aerobic oxidation of aldehydes (Boh et al., 1982; Nantes et al., 1995).

There is an ongoing debate in the scientific community whether ultra-weak chemiluminescence bears any functional relevance in biological organisms. The majority regards ultra-weak chemiluminescence as a waste product of the cell's metabolism. In contrast, some groups speculated whether ultra-weak chemiluminescence could trigger photochemical reactions within the cell (Cilento, 1982). Others even postulated that ultra-weak chemiluminescence is used for some kind of signalling or information transport in organisms, designating ultra-weak chemiluminescence as "biophotons" (e.g. Mei, 1994).

Most studies on ultra-weak chemiluminescence have investigated the nature of the light-generating chemical reactions (Allen, 1982; Cadenas, 1988; Cilento and Adam, 1995) and how diverse parameters (e.g. specific substrates, temperature) influence the quantity and quality of ultra-weak chemiluminescence (Boh et al., 1982; Hideg and Björn, 1996; Nantes et al., 1995). However, to our knowledge no studies about the propagation of emitted light within cells has been published. In the following, we present a theoretical analysis of the optical properties of different cell compartments. Based on this analysis, we propose a new view on the propagation of electromagnetic radiation und thus also ultra-weak chemiluminescence within biological tissues. We will focus on filamentous mitochondria with cross-striated cristae morphologies, which are typical for vertebrates. First we show that filamentous mitochondria and microtubules can act as optical waveguides (Section 2), then we analyse the optical properties of the different mitochondrial compartments (Section 3) and show the implications for the light propagation of intramitochondrial-generated chemiluminescence (Section 4). A general discussion concludes the article (Section 5).

2. Filamentous mitochondria and microtubules act like optical waveguides

An important optical property for the propagation of light within media is the index of refraction n. It

determines the propagation velocity v of electromagnetic waves within these media as $v = n^{-1}\, c$, where c represents the vacuum propagation velocity. Phase microscopy allows the measurement of the index of refraction for different intracellular components (Spencer, 1982). Measurements yielded values of $n_{cyto} = 1.35$ (Johnsen and Widder, 1999) for the cytoplasm and $n_{mito} = 1.4$ for whole mitochondria (Beuthan et al., 1996). For comparison, pure water has an index of refraction of 1.33. The optical geometry of a typical filamentous mitochondrion can thus be regarded as an elongated cylinder with a diameter of 300 nm, which is surrounded by a medium with a lower index of refraction. This configuration is analogous to fiber-optic waveguides, which allow the transmission of light along bent paths (Lipson et al., 1995). Fiber-optic waveguides consist of a cylindrical inner core surrounded by the cladding, which shows a lower index of refraction than the core material (Fig. 2A, B). The working principle of fiber-optic waveguides is based on total internal reflection, which is given if light approaches an interface towards a region with a lower index of refraction at an angle θ, which is smaller than the critical angle θ_{total} given as

$$\sin\theta_{total} = \left(1 - \frac{n_{core}^2}{n_{clad}^2}\right)^{1/2}, \tag{1}$$

where n_{core} and n_{clad} are the indices of refraction of the core and the cladding, respectively (Lipson et al., 1995).

A detailed theoretical analysis of the propagation of light within waveguides shows, that there exists only a discrete set of electromagnetic field patterns—termed "modes"—for high transmittance of electromagnetic waves through waveguides. The number of modes decreases with decreasing core diameter, but there remains always at least a single mode. Consequently, even waveguides with a core diameter much smaller than the wavelength of the light are able to guide light efficiently. For a given core diameter a cut-off wavelength (all wavelengths are regarded as vacuum wavelength), λ_c, can be calculated as

$$\lambda_c = 1.305\, D(n_{core}^2 - n_{clad}^2)^{1/2}, \tag{2}$$

where D represents the core diameter. There exists only a single mode for wavelengths longer than the cut-off wavelength λ_c (Lipson et al., 1995).

Electromagnetic radiation which is transmitted along fiber-optic waveguides is not totally confined to the inner core, but it is partly also located as an "evanescent field" in the surrounding cladding. The intensity I of the evanescent field decreases exponentially with increasing distance to the core center (Fig. 2C) as given by

$$I \sim \exp(-2\beta r), \tag{3}$$

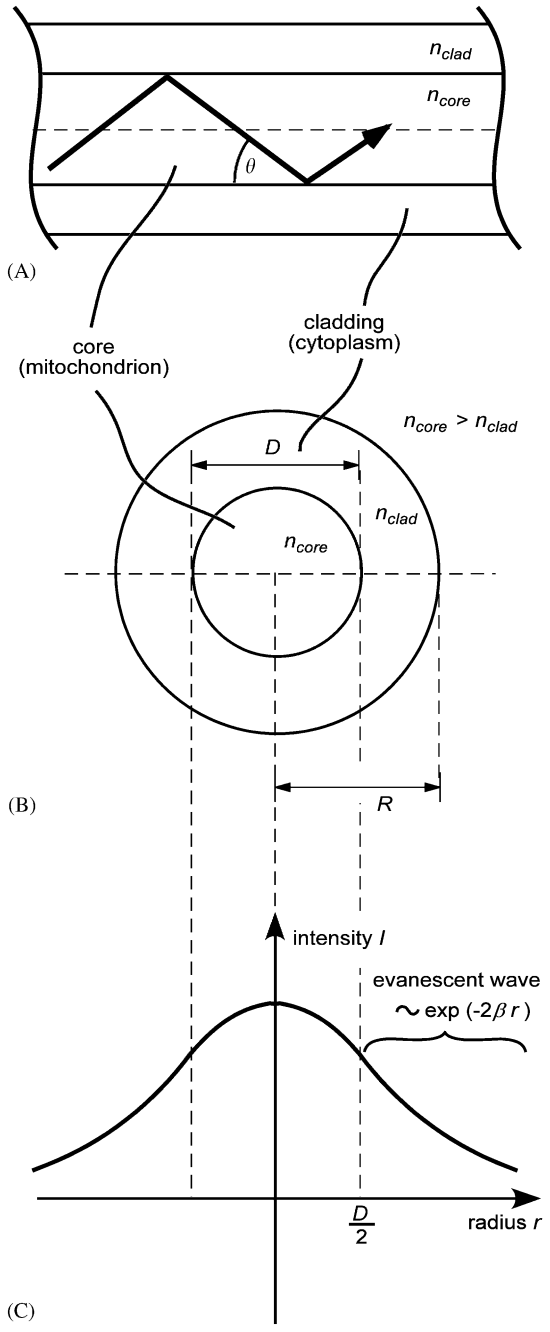

Fig. 2. Fiber-optic waveguide. (A) Longitudal cross-section. (B) Transversal cross-section. (C) Radial dependence of the electromagnetic field intensity.

where r is the distance from the core center and β lies in the range of

$$2\pi\, n_{core}\lambda^{-1} < \beta < 2\pi\, n_{clad}\lambda^{-1}, \tag{4}$$

where λ is the wavelength of the transmitted light. In order to assure a high transmittance of radiation along the fiber-optic waveguide, the radius R of the cladding has to be large enough in order to contain several decay lengths $(2\beta)^{-1}$ of the evanescent field

(Lipson et al., 1995):

$$R \gg (2\beta)^{-1}. \quad (5)$$

All the mentioned considerations, which are well established in the theory for light propagation in fiber-optic waveguides, can also be applied to mitochondria. Filamentous mitochondria themselves correspond to the fiber core with a typical diameter of $D = 300$ nm and $n_{core} = n_{mito} = 1.4$. The cytoplasm surrounding the mitochondria corresponds to the cladding with $n_{clad} = n_{cyto} = 1.35$. Using Eqs. (1) and (2) this gives a critical angle $\theta_{total} = 15.4°$ and a cut-off wavelength of $\lambda_c = 145$ nm. Thus, mitochondria could in principle act like single mode fibers for electromagnetic radiation with wavelengths > 145 nm, which comprises UV, visible, and NIR radiation. If we assume a typical wavelength in the visible region of $\lambda = 500$ nm, the decay lengths $(2\beta)^{-1}$ of the evanescent field will be ca. 30 nm following Eqs. (3) and (4). Filamentous mitochondria observed in the different cell types listed in the introduction are generally surrounded within several micrometer distance by cytoplasm, which means that Eq. (5) is satisfied. Therefore, filamentous mitochondria should in principle be able to act like waveguides along their long axis.

The same considerations also hold for the microtubules, which are composed of tubulin proteins arranged in a hollow cylinder 24 nm in diameter. The refractive index of microtubules was measured to be $n_{mt} = 1.51$ (Sato et al., 1975). Following the same reasoning as for light propagation in mitochondria, microtubules should also act as single mode waveguides.

The transmittance of light within mitochondria is in principle not confined to a single mitochondrion. Filamentous mitochondria forming an intracellular reticulum are often observed to be in close connection to each other, i.e. several mitochondria are arranged in a cable-like structure (Fig. 1) (Bakeeva et al., 1978; Bereiter-Hahn and Vöth, 1994; De Giorgi et al., 2000; Dedov and Roufogalis, 1999; Kirkwood et al., 1986; Poot et al., 1996; Shimada et al., 1984). The distance between neighbouring mitochondria is often much less than the wavelength of visible light and this would allow radiation propagating through a mitochondrion to cross the gap to a neighbouring mitochondrion where it can propagate further (Lipson et al., 1995). Additionally, the attachment of filamentous mitochondria with the microtubules of the cytoskeleton (Ball, 1982; Heggeness et al., 1978) can be optically described as two parallel waveguides in close proximity. The above calculated decay length of the evanescent field of ca. 30 nm enables electromagnetic waves propagating within a mitochondrion to be coupled via the evanescent field into the microtubule. Thus, even if filamentous mitochondria are not in close contact to each other, microtubules could provide light guiding along the cellular network of microtubules and filamentous mitochondria.

3. Mitochondria as an optical multi-layer system

The outer and inner membranes divide a mitochondrion into two compartments: the intramembrane space and the matrix (Fig. 3). The inner mitochondrial membrane in vertebrate cells generally exhibits cristae perpendicular to the long axis of the mitochondrion with fairly regular distances d between neighbouring

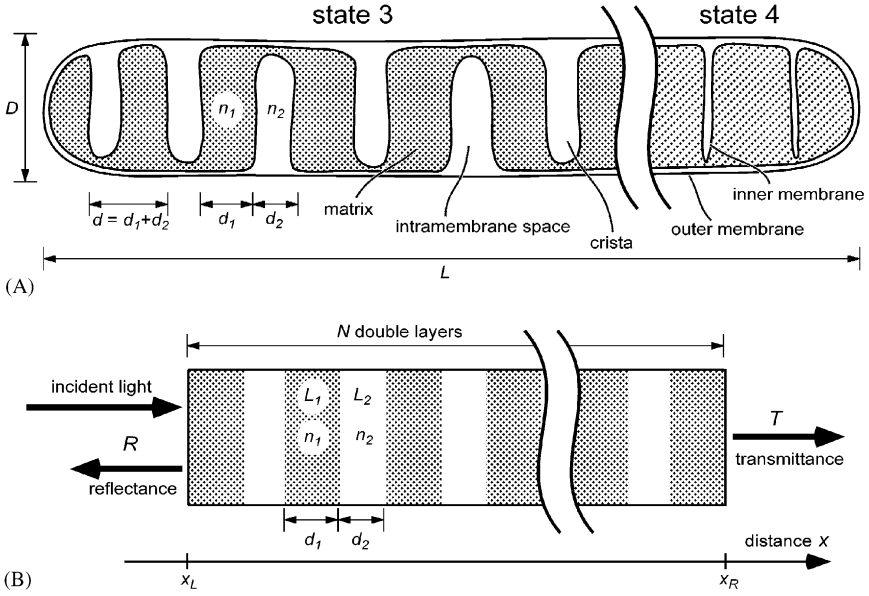

Fig. 3. (A) Internal organisation of filamentous mitochondrion with lamellar cristae. The left side shows state 3-, the right side state 4-configuration (B) Model of filamentous mitochondrion used for optical calculations. L length, D diameter of mitochondrion, d_1/n_1 thickness and refractive index of matrix space between two cristae, d_2/n_2 thickness and refractive index of cristae, N number of double layers, R reflectance, T transmittance.

Table 1
Protein content, refractive index, and thickness for the different compartments of the model mitochondrion with lamellar cristae as used for the optical calculations

	State 4 (resting)		State 3 (respiring)	
	Matrix + inner membrane	Intramembrane space	Matrix + inner membrane	Intramembrane space
Protein concentration ($g\,ml^{-1}$)	0.5	0.5	0.9	0.1
Index of refraction	$n_1 = 1.43$	$n_2 = 1.43$	$n_1 = 1.50$	$n_2 = 1.35$
Thickness (nm)	$d_1 = 90$	$d_1 = 10$	$d_1 = 50$	$d_1 = 50$

cristae. A filamentous mitochondrion thus appears in electron microscopic images as cross-striated with alternating layers of matrix and intramembrane space. A typical value for the distance d is about 100 nm, and this value will be used in the following calculations, although especially mitochondria in heart muscle tissue show values as low as 50 nm (Fawcett, 1981; Tandler and Hoppel, 1972). Advanced electron microscopy techniques have recently revealed that the actual morphology of the cristae is more complicated than given in the schematical drawing of Fig. 3 (Frey and Manella, 2000; Perkins and Frey, 2000). However, for our optical considerations the simplified model should give results, which are also valid for the actual more complex morphology.

The ratio between the volume of the matrix and the one of the intramembrane space is dependent on the physiological state of the mitochondrion. Provided that the mitochondrion is supplied with sufficient organic substrate and molecular oxygen, two states can be distinguished. At low ADP concentrations the mitochondria are in a resting state with low oxygen consumption, whereas at high ADP concentrations the mitochondria respire oxygen at their full capacity. Both states are traditionally termed state 4 and state 3, respectively (Hackenbrock, 1972). During state 4 the matrix occupies about 90% of the mitochondrial volume, i.e. the cristae appear as thin infoldings. On the transition to state 3 the cristae swell until the matrix volume is finally almost halved, i.e. mitochondria in state 3 show an approximately equal distribution between the matrix and the intramembrane space volume (Halestrap, 1989; Srere, 1980). The resultant state dependent thicknesses for the matrix layers, d_1, and for the intramembrane space layers, d_2, of a typical mitochondrion are listed in Table 1.

The numerous enzymes present in mitochondria result in a high protein concentration. The mitochondrial compartments differ considerably in their respective protein content. The matrix together with the inner membrane contain up to 90% of total mitochondrial protein, i.e. less than 10% are located in the intramembrane space (Schnaitman and Greenawalt, 1968). Thus, the matrix of mitochondria in state 4 show protein concentrations of up to $0.5\,g\,ml^{-1}$ (Hackenbrock, 1968; Srere, 1980), as can be anticipated by the electron dense appearance of the matrix in electron microscopic images. The almost two-fold contraction of the matrix volume during state 3 of respiring mitochondria increases the protein concentration further to up to $1\,g\,ml^{-1}$ (Srere, 1980). It can be calculated that such a high protein concentration approaches the densest possible packaging possible for protein molecules with minimal water content (Srere, 1980). The protein content influences the optical properties of the compartments. The index of refraction n is linearly dependent on the protein concentration as given by

$$n = 1.33 + 0.19\ c_{protein}, \tag{6}$$

where $c_{protein}$ is the protein concentration in units of $g\,ml^{-1}$ (Spencer, 1982). This dependency can now be applied to the known protein concentration of the different mitochondrial compartments (Table 1).

Mitochondria in the resting state 4 show no significant differences in the refractive indices of the intramembrane space and the matrix. Thus, they will act like homogeneous fiber-optic waveguides as described in the previous section. But the picture is different for actively respiring mitochondria in state 3. The matrix shows now an index of refraction as high as 1.5, which is comparable to values measured for certain glass types. In contrast, the index of refraction of the intramembrane space is about 1.35.

Based on the obtained information about the dimensions and the optical properties of the mitochondrial compartments during state 3, we formulated a one-dimensional optical model of an ideal mitochondrion. A mitochondrion can be represented as a multi-layer system of two alternating layers L_1 and L_2 with a thickness of d_1 and d_2 and an index of refraction of n_1 and n_2, respectively (Fig. 3B). Such an optical configuration corresponds to interference mirrors, which in case of perpendicular incident light show highest reflectivity for the wavelength

$$\lambda = (n_1 + n_2)d, \tag{7}$$

where $d = d_1 + d_2$ is the thickness of a single double layer (Fig. 3). Following the values given in Table 1,

Table 2
Reflectance R (see Fig. 2) of model mitochondrion with varying length L and number of double layers N

L (μm)	0.1	0.2	0.5	1	2	3	4	5
N	1	2	5	10	20	30	40	50
R (%)	1.10	4.31	23.32	61.34	94.26	99.28	99.91	99.99

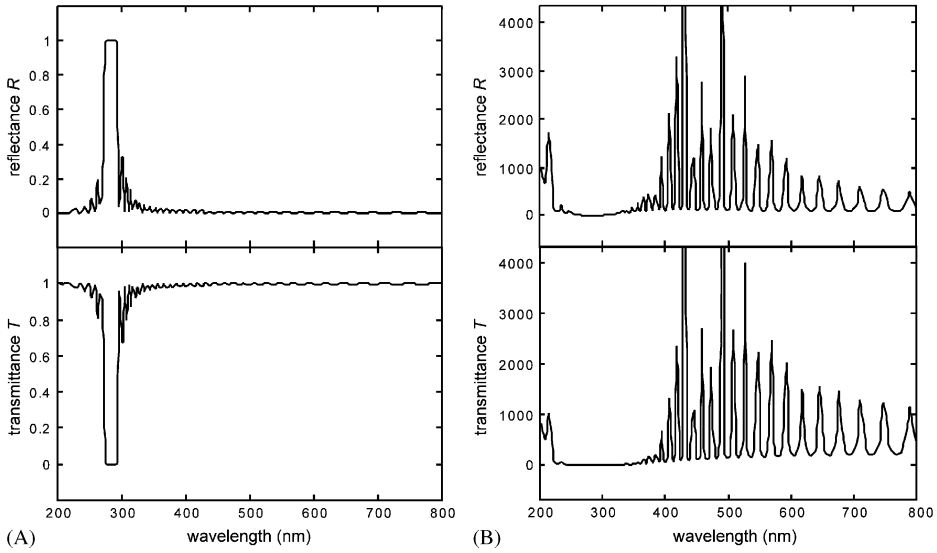

Fig. 4. Spectral reflectance and transmittance as calculated for model mitochondrion measuring 5 μm in length. (A) No amplification ($a=0$). (B) With amplification ($a=0.6\,\mu m^{-1}$).

mitochondria in state 3 should possess highest reflectivity at a wavelength of ca. 285 nm, if the incident light is directed as indicated in Fig. 3B. The absolute value of the reflectance R for this wavelength is dependent on the number of double layers and can be calculated by

$$R = \left(\left(\frac{n_2}{n_1}\right)^{2N} - 1\right)^2 \left(\left(\frac{n_2}{n_1}\right)^{2N} + 1\right)^{-2}, \quad (8)$$

where N is the number of double layers. A filamentous mitochondrion $L=1\,\mu m$ in length (N=10) shows a reflectivity of $R=61.34\%$, which increases to $R=99.99\%$ for a length of $L=5\,\mu m$ (N=50) (Table 2).

4. Spectral analysis of light propagation in mitochondria

The spectral dependencies of the transmittance T and the reflectance R in the one-dimensional optical model (Fig. 3B) can be analysed by the transfer-matrix method (see Appendix) (Lipson et al., 1995), which is generally applied for analysing optical multi-layer systems, e.g. interference filters. Additionally, we assumed a possible light amplification mechanism, i.e. electromagnetic waves travelling the distance Δx within the multi-layer system are amplified by the factor $\exp(a\,\Delta x)$, where a is the amplification constant (Eq.(A.4)). The intention behind this will be discussed later. The transfer-matrix method was implemented in a Mathematica program (Wolfram Research Inc.), which calculates the reflectance R and transmittance T for 200 different equidistant wavelengths λ within the interval of 200–800 nm.

Assuming an ideal filamentous mitochondrion ($D=300$ nm, $L=5\,\mu m$, $N=50$) in the respiring state 3 (Table 1) and no amplification ($a=0$), the resultant reflectance and transmittance spectra show a stop-band with almost unity reflectance ($R\approx100\%$) at the wavelengths of 270–290 nm (Fig. 4A), which is in accordance to the results of the previous section. In contrast, the wavelength region 300–800 nm shows almost unity transmittance ($T\approx100\%$) and an ideal filamentous mitochondria in both metabolic states 3 and 4 should for these wavelengths act like fiber-optic waveguides if neither light amplification nor absorption is assumed.

A different result is obtained if we assume that the electromagnetic waves can be amplified when propagating through the mitochondrion, i.e. $a>0$ (Eq. (A.4)). Assuming otherwise the same parameters as before, the resultant reflectance and transmittance spectra show a series of peaks within the range of visible light (Fig. 4B). For example if we choose $a=0.6\,\mu m^{-1}$ (unfortunately, there are no experimental data so far available in order

to obtain a quantitative estimate for a), light of unity intensity entering the ideal mitochondrion from the left side is amplified at the peak wavelengths up to 10000 times and is emitted almost symmetrical towards both sides of the mitochondrion as can be anticipated from the transmittance and reflectance spectra. Most of the emitted light energy now originate from the amplification mechanism inside the ideal mitochondrion, as the incident light intensity measures only a fraction of the emitted one.

The latter results were obtained by assuming an external incident light source of unity intensity from the left side (Fig. 3B), which initiated the amplification process. In case the external light source is replaced by an internal light source within the first layer to the left side, this source would initiate still the same amplification process, i.e. it will result in emission spectra to the left and the right end of the multi-layer system which are identical to the reflectance and transmittance spectra in Fig. 4B, respectively. Furthermore, the almost symmetrical shape of both spectra indicates that the actual position of the internal source should not affect the qualitative shape of the resultant emission spectra. Thus, an ideal filamentous mitochondrion in state 3, which generates chemiluminescence and additionally exhibits the proposed amplification mechanism could emit light at both ends with characteristic peaks in the spectral light composition.

Chemiluminescence from mitochondria originates generally from excited molecules generated by the oxidative metabolism of mitochondria. There exist two principal mechanisms for photon emission from an excited molecule: spontaneous and induced emission (Lipson et al., 1995). In the first case, the excited molecules emit the photons with a certain decay rate. Assuming that the excited molecules have a random spatial orientation, the emitted photons will not exhibit a preferred propagation direction, i.e. the emission is isotropic. The angle, θ, between the propagation direction and the long axis of an ideal mitochondrion determines whether the emitted photon is actually "captured" within the mitochondrion and guided by the optical properties of the mitochondrion (see Section 2). According to Eq. (1), only photons with an angle θ smaller than the critical angle θ_{total} will be captured and propagate along an ideal mitochondrion. Assuming an isotropic emission characteristic, the fraction f of captured photons can be calculated as

$$f = (1 - \cos\theta_{total}) \tag{9}$$

which gives $f = 0.036$ if we assume $\theta_{total} = 15.4^\circ$ (Section 2). Thus, only 3.6% of the emitted photons are actually captured within an ideal mitochondrion and guided towards both its ends.

In the second case, induced emission provides a possible mechanism for the proposed amplification of the internal light field. Induced emission takes place when an excited molecule is hit by a photon inducing the emission of a second photon. Both photons have identical propagation directions and phase relations, which was the underlying assumption for the mathematical formulation of the amplification process in Eq. (A.4). If induced photon emission is predominant over spontaneous emission, the fraction f of the captured and guided light changes significantly. Captured photons, which are guided along an ideal filamentous mitochondrion, would have a longer residence time within the mitochondrion than non-captured photons. Thus, induced emission will predominantly take place for captured photons. This results in a self-amplification process providing that the fraction f of captured photons approaches 100%. The emitted light should show temporal coherence as photons generated by induced emission have identical phases.

The spectra shown in Fig. 4B were calculated with the assumption of a wavelength-independent amplification constant a. In reality, the self-amplification mechanism of induced photon emission will cause the amplification process to select for specific peaks within these spectra. Which peaks are actually selected depends on the emission spectrum of the excited molecule. Chemiluminescence from mitochondria has been detected within the visible region of the electromagnetic spectrum (Boh et al., 1982; Hideg et al., 1991; Nantes et al., 1995), thus, it is likely that also peaks within this region are selected. Consequently, if induced emission actually is the dominant emission process within filamentous mitochondria in metabolic state 3, the internally generated light will be emitted at both ends of the mitochondria with high temporal coherence and high directivity, i.e. mitochondria would act like lasers. The described lasing principle has been technically realized in the design of distributed feedback lasers, which consist of a similar multi-layer system consisting of layers with different indices of refraction (Kneubühl and Sigrist, 1999).

5. Discussion

Most of the presented considerations are well supported by optical theory, but we are aware that the assumption of induced light emission is very speculative. The internal light intensity of technical lasers has to be above a certain threshold in order for the induced light emission to predominate the spontaneous one (Kneubühl and Sigrist, 1999). Typical threshold light intensities are many orders of magnitude higher than the intensity of ultra-weak chemiluminescence. Thus, it appears to be very unlikely that induced light emission takes place in mitochondria. However, there are some points to be considered: Due to the optical waveguide properties of the mitochondrial network, only a small fraction of the

internal light field might actually leave the network. Thus, the actual light intensity inside the mitochondria might be considerably higher than one would expect from the measurements on ultra-weak chemiluminescence, which is generally measured macroscopically several centimetres in distance from the tissue or cell cultures (Cadenas, 1988; Inaba, 1988; Mei, 1994). Furthermore, in recent years technical micro-lasers have been manufactured approaching the small dimensions of mitochondria. It has been shown that the threshold light intensity for these micro-lasers is significantly lower than observed for macroscopic lasers (e.g. Loncar et al., 2002). Altogether, there are too many unknown parameters at the current stage in order to evaluate quantitatively the possibility of induced light emission within mitochondria.

Nevertheless, we have shown that the mitochondrial network within eukaryotic cells possesses optical properties, which to our knowledge have so far not been considered regarding the light propagation within eukaryotic cells and tissues. Most treatise on this subject are based on scattering theory, assuming that the light propagation is mainly based on random absorption and scattering events (e.g. Yamada, 2000). In contrast, the demonstrated light guiding properties of the mitochondrial network indicate that the light propagation can be essentially non-random. It is tempting to speculate whether this is related to any biological function.

Cilento has pointed to the possibility that biochemically generated excited molecules could transfer their energy to other molecules, where it in turn triggers chemical reactions (Cilento, 1982). Whereas Cilento considered interactions of molecules in close contact to each other, the mechanism could be extended to long-range interactions if the light guiding properties of the mitochondrial network are additionally taken into account. Chemiluminescent light generated in one mitochondrion could propagate along the network and, e.g., trigger some chemical reaction in another mitochondrion. This picture would provide that the physiology of mitochondria can be effected by light illumination. Interestingly, there exists a wealth of experimental data about the influence of low power laser irradiation on cell cultures (e.g. Alexandratou et al., 2002; Kaku, 1990; Karu et al., 2001; Schwartz et al., 2002; Shefer et al., 2002). Typical experiments were based on daily short-period illumination of cell cultures with a certain visible light dose, which resulted in significant changes in the physiology and proliferation of cells. Pathologic effects could be excluded as the observed effects were strictly dose-dependent, i.e. there existed an optimum daily light dose, which showed the most prominent effect on the cell cultures. It is presumed that the site of the interaction between the light field and the cells was located within the mitochondria, and indeed experiments with isolated mitochondria demonstrated that external illumination influenced their physiology significantly (Breitbart et al., 1996; Gordon and Surrey, 1960; Greco et al., 2001; Kato et al., 1981; Morimoto et al., 1994; Passarella et al., 1984).

Altogether, we know that mitochondria emit chemiluminescent light, we know that their physiology is influenced by illumination, and our present study shows that light can be guided along the mitochondrial network. Thus, it is very tempting to speculate whether there exists in reality some long-range interaction between individual mitochondria, which is mediated by electromagnetic radiation. The biological function and relevance of this possible mechanism would be the next question to be answered.

Acknowledgements

We would like to thank Willfried Staude for advice regarding the transfer matrix method, and Ian Max Møller for commenting an earlier version of the manuscript. Andrea Wieland, Konstantin Boucke, and Karen Willbrand inspired by fruitful discussions. This study was supported by the EU-project PHOBIA (QRLT-2001-01938) to RT and by the Danish Natural Science Research Council (Contract 9700549) to MK.

Appendix. A

One-dimensional electromagnetic waves with wavelength λ in the optical multi-layer system (Fig. 3B) can be described by the electric field E of two waves travelling in opposite direction (Lipson et al., 1995). The electrical field E along the x-axis at time t is then given as

$$E(x,t) = \mathrm{Re}\left\{(\mathbf{E}^+(x) + \mathbf{E}^-(x))\exp\left(\mathrm{i}\frac{2\pi c}{\lambda}t\right)\right\}, \qquad (A.1)$$

where $\mathrm{i} = \sqrt{-1}$, c is the vacuum speed of light, and $\mathrm{Re}\{Z\}$ returns the real part of its complex argument Z. $\mathbf{E}^+(x)$ and $\mathbf{E}^-(x)$ are the time-independent complex amplitudes of the electric fields belonging to the waves propagating into positive and negative x-direction, respectively. The complex amplitude is defined as $\mathbf{E} = E\exp(\mathrm{i}\varphi)$ where E is the amplitude and φ the phase of the electric field wave. We assume normal incident waves and regard only one polarization direction. Thus, the electromagnetic field at position x for a given wavelength λ can be described by the time-independent complex state vector

$$\vec{\mathbf{E}}(x) = \begin{pmatrix} \mathbf{E}^+(x) \\ \mathbf{E}^-(x) \end{pmatrix}. \qquad (A.2)$$

If the state vector is known at a single position x, the state vectors at all other positions can be calculated by

the transfer-matrix method. The state vector to the right side x_R of the multi-layer system is related to the one to the left side x_L by

$$\vec{\mathbf{E}}(x_R) = (\mathbf{T}_{21}\mathbf{S}_2\mathbf{T}_{12}\mathbf{S}_1)^N \vec{\mathbf{E}}(x_L), \tag{A.3}$$

where $\mathbf{S}_k$ is the transfer matrix for the transition of the state vector inside a layer L_k given by

$$\mathbf{S}_k = \begin{pmatrix} \exp\left(-\mathrm{i}n_k\frac{2\pi}{\lambda}d_k\right)\exp(ad_k) & 0 \\ 0 & \exp\left(\mathrm{i}n_k\frac{2\pi}{\lambda}d_k\right)\exp(-ad_k) \end{pmatrix}. \tag{A.4}$$

The constant a represents a possible amplification of the electromagnetic wave crossing a layer L_k with thickness d_k and an index of refraction n_k. The electromagnetic waves will be partially reflected at the boarder of adjacent layers L_k and L_l due to their different indices of refraction ($n_k \neq n_l$). This process is represented by the transfer matrix $\mathbf{T}_{kl}$:

$$\mathbf{T}_{kl} = \frac{1}{2}\begin{pmatrix} 1+\frac{n_k}{n_l} & 1-\frac{n_k}{n_l} \\ 1-\frac{n_k}{n_l} & 1+\frac{n_k}{n_l} \end{pmatrix}. \tag{A.5}$$

Assuming an incident wave of unity intensity from the left side, the following boundary conditions can be applied:

$$\vec{\mathbf{E}}(x_L) = \begin{pmatrix} 1 \\ \mathbf{E}^-(x_L) \end{pmatrix} \quad \text{and} \quad \vec{\mathbf{E}}(x_R) = \begin{pmatrix} \mathbf{E}^+(x_R) \\ 0 \end{pmatrix} \tag{A.6}$$

which are satisfactory in order to solve Eq. (A.3) for $\mathbf{E}^-(x_L)$ and $\mathbf{E}^+(x_R)$. As the light intensities are proportional to the square of the amplitude of the electric fields, the reflectance R and the transmittance T are given by

$$R = (\mathbf{E}^-(x_L))^2 \quad \text{and} \quad T = (\mathbf{E}^+(x_R))^2. \tag{A.7}$$

References

Adam, W., Cilento, G. (Eds.), 1982. Chemical and Biological Generation of Excited States. Academic Press, New York.

Alexandratou, E., Yova, D., Handris, P., Kletsas, D., Loukas, S., 2002. Human fibroblast alterations induced by low power laser irradiation at the single cell level using confocal microscopy. Photochem. Photobiol. Sci. 1 (8), 547–552.

Allen, R.C., 1982. Biochemiexcitation: Chemiluminescence and the study of biological oxygenation reactions. In: Adam, W., Cilento, G. (Eds.), Chemical and Biological Generation of Excited States. Academic Press, New York.

Bakeeva, L.E., Chentsov Yu, S., Skulachev, V.P., 1978. Mitochondrial framework (reticulum mitochondriale) in rat diaphragm muscle. Biochim. Biophys. Acta 501 (3), 349–369.

Ball, E.H., 1982. Mitochondria are associated with microtubules and not with intermediate filaments in cultured fibroblasts. Proc. Natl Acad. Sci. USA 79, 123–126.

Barja, G., 1999. Mitochondrial oxygen radical generation and leak: sites of production in states 4 and 3, organ specificity, and relation to aging and longevity. J. Bioenerg. Biomembr. 31 (4), 347–366.

Bereiter-Hahn, J., 1990. Behavior of mitochondria in the living cell. Int. Rev. Cytol. 122, 1–63.

Bereiter-Hahn, J., Vöth, M., 1994. Dynamics of mitochondria in living cells: shape changes, dislocations, fusions, and fissions of mitochondria. Microscopy Res. Tech. 27, 198–219.

Beuthan, J., Minet, O., Helfmann, J., Herrig, M., Muller, G., 1996. The spatial variation of the refractive index in biological cells. Phys. Med. Biol. 41 (3), 369–382.

Boh, E.E., Baricos, W.H., Bernofsky, C., Steele, R.H., 1982. Mitochondrial chemiluminescence elicited by acetaldehyde. J. Bioenerg. Biomembr. 14 (2), 1982.

Breitbart, H., Levinshal, T., Cohen, N., Friedmann, H., Lubart, R., 1996. Changes in calcium transport in mammalian sperm mitochondria and plasma membrane irradiated at 633 nm (HeNe laser). J. Photochem. Photobiol. B 34 (2–3), 117–121.

Cadenas, E., 1988. Biological chemiluminescence. NATO ASI Ser, Ser. A 146, 117–141.

Cilento, G., 1982. Electronic excitation in dark biological processes. In: Adam, W., Cilento, G. (Eds.), Chemical and Biological Generation of Excited States. Academic Press, New York.

Cilento, G., Adam, W., 1995. From free radicals to electronically excited species. Free Radical Biol. Med. 19 (1), 103–114.

De Giorgi, F., Lartigue, L., Ichas, F., 2000. Electrical coupling and plasticity of the mitochondrial network. Cell Calcium 28 (5–6), 365–370.

Dedov, V.N., Roufogalis, B.D., 1999. Organisation of mitochondria in living sensory neurons. FEBS Lett. 456, 171–174.

Droge, W., 2002. Free radicals in the physiological control of cell function. Physiol. Rev. 82 (1), 47–95.

Fawcett, D., 1981. The Cell. Saunders, Philadelphia.

Frey, T., Manella, C., 2000. The internal structure of mitochondria. Trends Biochem. Sci. July, 319–324.

Gordon, S., Surrey, K., 1960. Red and far-red action on oxidative phosphorylation. Radiat. Res. 12, 325–339.

Greco, M., Vacca, R.A., Moro, L., Perlino, E., Petragallo, V.A., Marra, E., Passarella, S., 2001. Helium–neon laser irradiation of hepatocytes can trigger increase of the mitochondrial membrane potential and call stimulate c-fos expression in a Ca2+-dependent manner. Laser Surg. Med. 29 (5), 433–441.

Hackenbrock, C.R., 1968. Chemical and physical fixation of isolated mitochondria in low-energy and high-energy states. Proc. Natl Acad. Sci. USA 61 (2), 598–605.

Hackenbrock, C.R., 1972. States of activity and structure in mitochondrial membranes. Ann. NY Acad. Sci. 195, 492–505.

Halestrap, A.P., 1989. The regulation of the matrix volume of mammalian mitochondria in vivo and in vitro and its role in the control of mitochondrial metabolism. Biochim. Biophys. Acta 973 (3), 355–382.

Heggeness, M.H., Simon, M., Singer, S.J., 1978. Association of mitochondria with microtubules in cultured cells. Proc. Natl Acad. Sci. USA 75 (8), 3863–3866.

Hideg, É., Björn, L., 1996. Ultraweak light emission, free radicals, chilling and light sensitivity. Physiol. Plantarum 98, 223–228.

Hideg, È., Kobayashi, M., Inaba, H., 1991. Spontaneous ultraweak light emission from respiring spinach leaf mitochondria. Biochim. Biophys. Acta 1098, 27–31.

Inaba, H., 1988. Super-high sensitivity systems for detection and spectral analysis of ultraweak photon emission from biological cells and tissues. Experientia 44 (7), 550–559.

Johnsen, S., Widder, E.A., 1999. The physical basis of transparancy in biological tissue: ultrastructure and the minimization of light scattering. J. Theor. Biol. 199, 181–198.

Kaku, T., 1990. Effects of visible radiation on cultured cells. J. Photochem. Photobiol. 52 (6), 1089–1099.

Karu, T.I., Pyatibrat, L.V., Kalendo, G.S., 2001. Donors of NO and pulsed radiation at lambda = 820 nm exert effects on cell attachment to extracellular matrices. Toxicol. Lett. 121 (1), 57–61.

Kato, M., Shinzawa, K., Yoshikawa, S., 1981. Cytochrome oxidase is a possible photoreceptor in mitochondria. J. Photochem. Photobiol. 2, 263–269.

Kirkwood, S.P., Munn, E.A., Brooks, G.A., 1986. Mitochondrial reticulum in limb skeletal muscle. Am. J. Physiol. 251 (3 Pt 1), C395–C402.

Kneubühl, F.K., Sigrist, M.W., 1999. Laser. Teubner, Stuttgart.

Lipson, S.G., Lipson, H.S., Tannhauser, D.S., 1995. Optical Physics, 3rd Edition. Cambridge University Press, Cambridge.

Loncar, M., Yoshie, T., Scherer, A., Gogna, P., Qiu, Y.M., 2002. Low-threshold photonic crystal laser. Appl. Phys. Lett. 81 (15), 2680–2682.

Mei, W., 1994. About the nature of biophotons. J Biol. Systems 2 (1), 25–42.

Mitchell, P., 1977. Vectorial chemiosmotic processes. Annu. Rev. Biochem. 46, 996–1005.

Møller, I.M., 2001. Plant mitochondria and oxidative stress: electron transport, NADPH turnover, and metabolism of reactive oxygen species. Annu. Rev. Plant. Physiol. Plant. Mol. Biol. 52, 561–591.

Morimoto, Y., Arai, T., Kikuchi, M., Nakajima, S., Nakamura, H., 1994. Effect of low-intensity argon-laser irradiation on mitochondrial respiration. Laser Surg. Med. 15 (2), 191–199.

Nantes, I.L., Cilentos, G., Bechara, E.J.H., Vercesi, A.E., 1995. Chemiluminescence diphenylacetaldehyde oxidation by mitochondria is promoted by cytochromes and leads to oxidative injury of the organelle. J. Photochem. Photobiol. 62 (3), 522–527.

Nieminen, A.L., 2003. Apoptosis and necrosis in health and disease: role of mitochondria. Int. Rev. Cytol. 224, 29–55.

Ohta, S., 2003. A multi-functional organelle mitochondrion is involved in cell death, proliferation and disease. Curr. Med. Chem. 10 (23), 2485–2494.

Passarella, S., Casamassima, E., Molinari, S., Pastore, D., Quagliariello, E., Catalano, I.M., Cingolani, A., 1984. Increase of proton electrochemical potential and atp synthesis in rat liver mitochondria irradiated in vitro by helium–neon laser. FEBS Lett. 175 (1), 95–99.

Perkins, G.A., Frey, T.G., 2000. Recent structural insight into mitochondria gained by microscopy. Micron 31 (1), 97–111.

Perkins, G., Renken, C., 1997. Electron tomography of neuronal mitochondria: three-dimensional structure and organization of cristae and membrane contacts. J. Struct. Biol. 119, 260–272.

Poot, M., Zhang, Y.-Z., Krämer, J.A., Wells, K.S., Jones, L.J., Hanzel, D.K., Lugade, A.G., Singer, V.L., Haugland, R.P., 1996. Analysis of mitochondrial morphology and function with novel fixable fluorescent stains. J. Histochem. Cytochem. 44 (12), 1363–1372.

Riva, A., Loffredo, F., Uccheddu, A., Riva, F.T., Tandler, B., 2003. Mitochondria of human adrenal cortex have tubular cristae with bulbous tips. J. Clin. Endocrinol. Metab. 88 (4), 1903–1906.

Sato, H., Ellis, G.W., Inoué, S., 1975. Microtubular origin of mitotic spindle form birefringence: demonstration of the applicability of Wiener's equation. J. Cell. Biol. 67, 501–517.

Schnaitman, C., Greenawalt, J.W., 1968. Enzymatic properties of the inner and outer membranes of rat liver mitochondria. J. Cell. Biol. 38 (1), 158–175.

Schwartz, F., Brodie, C., Appel, E., Kazimirsky, G., Shainberg, A., 2002. Effect of helium/neon laser irradiation on nerve growth factor synthesis and secretion in skeletal muscle cultures (vol 66, pg 195, 2002). J. Photoch. Photobiol. B 68(2–3), 165–165.

Shefer, G., Partridge, T.A., Heslop, L., Gross, J.G., Oron, U., Halevy, O., 2002. Low-energy laser irradiation promotes the survival and cell cycle entry of skeletal muscle satellite cells. J. Cell Sci. 115 (7), 1461–1469.

Shimada, T., Horita, K., Murakami, M., Ogura, R., 1984. Morphological studies of different mitochondrial populations in monkey myocardial cells. Cell. Tissue Res. 238 (3), 577–582.

Spencer, M., 1982. Fundamentals of Light Microscopy. Cambridge University Press, Cambridge.

Srere, P., 1980. The infrastructure of the mitochondrial matrix. Trends Biochem. Sci. 5, 120–121.

Tandler, B., Hoppel, C.L., 1972. Mitochondria. Academic Press, New York.

Turrens, J.F., 2003. Mitochondrial formation of reactive oxygen species. J. Physiol. 552 (Pt 2), 335–344.

Yamada, Y., 2000. Fundamental studies of photon migration in biological tissues and their application to optical tomography. Opt. Rev. 7 (5), 366–374.